

Passive Virtual Fixtures Based on Simulated Position-Dependent Anisotropic Plasticity

Ryo Kikuuwe, Naoyuki Takesue, and Hideo Fujimoto

Abstract—This paper presents an approach for producing virtual fixture based on simulated plasticity, which can be used for assisting precise manual manipulations performed by human users through haptic interfaces. The fixture acts as a guide to help path-tracing tasks and as a wall for preventing a tool from entering a specified region, but the user can move against the fixture by intentionally producing a force larger than a predetermined yield force. The advantage of the proposed virtual fixture is that it is always passive and it acts as a hard fixture when the user's force is smaller than the yield force. The algorithm was demonstrated through experiments using an impedance-type haptic interface.

I. INTRODUCTION

Humans are capable of intelligent and dexterous manual manipulation, but human voluntary motions are generally inaccurate due to low-frequency fluctuations such as physiological tremors. One approach for enhancing the accuracy of human manual manipulation is the use of a haptic interface for producing physical constraints like a ruler to draw a straight line with or a wall to keep the tool away from a hazardous area, as illustrated in Fig. 1. This kind of computer-generated constraint is often referred to as a virtual fixture. This approach can be viewed as a co-manipulation between a human and a robotic system and has been used for assisting precise manipulation such as micro surgery [1]–[3]. The virtual fixture approach can also be used in telemanipulation systems in hazardous environment [4]. This type of human-machine coordination schemes are especially useful in cases when the full automation is technically almost possible but is unacceptable due to reliability or economical reasons.

For ensuring safety and for preventing unexpected behavior of the haptic interface, a virtual fixture is preferred to be always passive. It is however not a trivial problem to produce an always-passive physical constraint with active haptic interfaces. For example, let us consider a hard elastic virtual wall to prevent the tool from entering a specified forbidden region. Since the computer-generated virtual fixture is not fully reliable, the human operator must be allowed to enter the forbidden region. When the user produces a large force to penetrate the virtual wall, a saturated elastic force will always act upon the tool as long as it is inside the forbidden region, and in this situation, the virtual wall is not passive anymore. Bettini et al. [2] constructed virtual fixture algorithms based on simulated viscosity, which produces always-passive resistance force. In their approach, the user's

motion in a forbidden direction is resisted by a large viscous resistance. A disadvantage of this approach may be that small and slow penetrations into the forbidden region are inevitable even if the user has no such intentions.

This paper presents an approach for producing virtual fixtures based on simulated *plasticity*. Here we use the term plasticity to mean the characteristic of an object whereby it produces a permanent displacement under a force larger than a particular value (a yield force) but it does not produce any motion under a force smaller than the yield force. The Coulomb friction is an example for this characteristic. A typical example of plastic response in the n -dimensional space can be described as follows:

$$\mathbf{f} = -F\dot{\mathbf{q}}/\|\dot{\mathbf{q}}\|, \quad (1)$$

where $\mathbf{f} \in \mathbb{R}^n$ and $\dot{\mathbf{q}} \in \mathbb{R}^n$ denote the resistance force and the velocity, respectively, and $F > 0$ denotes the yield force. The resistance force \mathbf{f} always opposes the velocity $\dot{\mathbf{q}}$ and thus the force is always passive. The force \mathbf{f} is discontinuous with respect to the velocity $\dot{\mathbf{q}}$ at $\dot{\mathbf{q}} = \mathbf{0}$ (hereafter $\mathbf{0}$ denotes the zero-vector of an appropriate dimension) and when $\dot{\mathbf{q}} = \mathbf{0}$, the force \mathbf{f} balances external forces to maintain zero velocity below the yield force F . Because of the discontinuous definition as in (1), the plasticity had been cumbersome to be implemented in discrete-time control systems. However, such difficulties have been removed by our recent achievement [5], which provides a mathematical framework for treating Coulomb-like friction in discrete time.

In the plasticity-based virtual fixture approach, the motion in a forbidden (non-preferred) direction is resisted by a large yield force. One advantage of a plasticity-based virtual fixture over a viscosity-based one [2] is that the user can distinguish the direction in which the tool should not move *before* it actually starts to move. The tool does not enter the forbidden region (strictly, is servoed on the boundary of the forbidden region) as long as the user force is below the yield force, and thus whether the direction is preferred or not can be recognized by whether the fixture yields or not. The initial idea of the plasticity-based virtual guide was

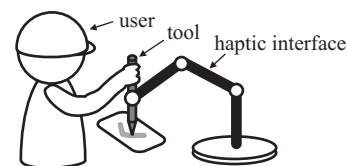


Fig. 1. A co-manipulation system.

The authors are with Nagoya Institute of Technology, Nagoya, Aichi 466-8555, Japan. E-mail: kikuuwe@ieee.org

presented in one of our previous papers [6], in which we proposed a “friction wall” for assisting precise trajectory-tracing tasks. However, its advantages were not explained or demonstrated enough and was limited to admittance-type haptic interfaces. Moreover, its algorithm was immature in that it produced remaining overshoots after crossing the trajectory to be traced. This paper aims to present overall improvements and extensions of the “friction wall” approach and to demonstrate its advantage.

The rest of this paper is organized as follows. Section II describes a simple one-dimensional, plasticity-based virtual fixture. Section III describes multidimensional algorithms. Section IV experimentally demonstrates the proposed algorithms by using an impedance-type haptic interface. Section V provides concluding remarks.

II. ONE-DIMENSIONAL VIRTUAL FIXTURES

A. Simulated Plasticity

We start our derivation from a simple one-dimensional model. The plasticity is the dynamics with which the motion does not occur with an external force smaller than a yield force level and the resistance force is constant at any non-zero velocity. Consider an object of which the position is denoted by q . The relation between the force and the motion can be described as follows:

$$f = -g\text{sgn}(-F, \dot{q}, F). \quad (2)$$

Here, $F > 0$ and we define $g\text{sgn}(a, x, b)$, a generalized signum function, as follows:

$$g\text{sgn}(a, x, b) \begin{cases} = b & \text{if } x > 0 \\ \in [a, b] & \text{if } x = 0 \\ = a & \text{if } x < 0. \end{cases} \quad (3)$$

Notice that f can take an arbitrary value between $-F$ and F when $\dot{q} = 0$. It has been difficult to use (2) for haptic rendering because the force f is indeterminate at $\dot{q} = 0$ and is discontinuous with respect to \dot{q} at $\dot{q} = 0$. For example, if the actuator force f is determined by using (2) with the measured velocity being used as \dot{q} , the haptic interface will exhibit high frequency oscillation due to repeated zero-velocity crossings.

The plastic response (2) can be implemented in haptic rendering systems by following the method presented in our

recent paper [5]. There are two types of haptic rendering schemes: the impedance type and the admittance type. In the impedance-type haptic rendering, the position p of the tool (haptic interface) is measured, the reaction force f from the virtual world is calculated, and the force f is commanded to the actuators. In the admittance-type scheme, the force h applied from the user is measured by force sensors, the position q of the virtual object in the virtual world is updated, and the tool position is controlled to follow the position q .

For simulating the plasticity in impedance-type haptic rendering, we must consider a massless virtual object (proxy), of which the position is denoted by q , in the software, as illustrated in Fig. 2(a). The proxy accepts the plastic force (2) and is connected to the tool through a virtual spring-damper element. The force from the virtual spring-damper element always balances the plastic force f in (2), and thus it can also be denoted by f . It satisfies

$$f = K(q - p) + B(\dot{q} - \dot{p}) \quad (4)$$

where K and B are the stiffness and viscosity coefficients of the virtual spring-damper element. In the admittance type, on the other hand, we must consider a virtual object having a non-zero mass M . We also call this object as a proxy hereafter. The input force h and the force f of (2) act to the proxy as shown in Fig. 2(b). Thus, the equation of motion of the proxy is written as

$$f = M\ddot{q} - h. \quad (5)$$

Based on the backward Euler scheme, (2), (4), and (5) can be rewritten as

$$f(i) = g\text{sgn}(-F, q(i-1) - q(i), F), \quad (6)$$

$$f(i) = K(q(i) - p(i)) + B(q(i) - q(i-1) - p(i) + p(i-1))/T, \quad (7)$$

$$f(i) = M(q(i) - 2q(i-1) + q(i-2))/T^2 - h(i), \quad (8)$$

respectively. Here, T is the timestep size and the arguments in the parentheses, such as i and $i-1$, are discrete time indices. Both of (7) and (8) can be rewritten as

$$f(i) = \kappa(q(i) - p^*(i)) \quad (9)$$

where

$$\kappa = K + B/T \quad (10)$$

$$p^*(i) = p(i) + B(q(i-1) - p(i-1))/(KT + B) \quad (11)$$

in the case of (7), the impedance type, and

$$\kappa = M/T^2 \quad (12)$$

$$p^*(i) = 2q(i-1) - q(i-2) + T^2 h(i)/M \quad (13)$$

in the case of (8), the admittance type. Substituting (6) into (9) yields

$$\kappa(q(i) - p^*(i)) = g\text{sgn}(-F, q(i-1) - q(i), F). \quad (14)$$

Note that $p^*(i)$ can be treated as a known variable because it only depends on past values and current input values, as indicated in (11) and (13). It can be interpreted as the

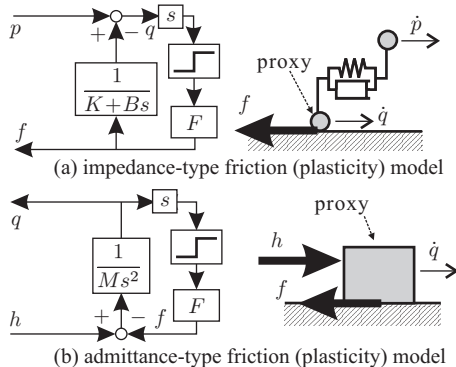


Fig. 2. Friction (plasticity) models for haptic rendering [5].

proxy position that could have been achieved if no plastic force acted. We hereafter refer to $p^*(i)$ as the *input position*. The use of a common form (9) for both admittance- and impedance-type haptic rendering schemes is detailed in [7].

The current proxy position $q(i)$ has to be determined so that it satisfies (14). A derivation detailed in [5] shows that the solution for (14) is

$$q(i) = \text{gsat}(p^*(i) - F/\kappa, q(i-1), p^*(i) + F/\kappa). \quad (15)$$

Here, $\text{gsat}(a, x, b)$ is a generalized saturation function defined as $\text{gsat}(a, x, b) = \max(a, \min(x, b))$, which returns x if $x \in [a, b]$ and returns the saturated value otherwise. This satisfies

$$\text{gsat}(a, x, b) = \lim_{c \rightarrow \infty} \text{gsat}(a, cx + d, b), \quad \forall d \in \mathbb{R}. \quad (16)$$

In conclusion, the computational procedure to realize plastic responses in the impedance-type haptic rendering is given as follows:

$$p^*(i) = p(i) + B(q(i-1) - p(i-1))/(KT + B) \quad (17)$$

$$q(i) = \text{gsat}(p^*(i) - F/\kappa, q(i-1), p^*(i) + F/\kappa) \quad (18)$$

$$f(i) = \kappa(q(i) - p^*(i)) \quad (19)$$

where $\kappa = K + B/T$. In the admittance type, on the other hand, it is given as

$$p^*(i) = 2q(i-1) - q(i-2) + T^2h(i)/M \quad (20)$$

$$q(i) = \text{gsat}(p^*(i) - F/\kappa, q(i-1), p^*(i) + F/\kappa) \quad (21)$$

where $\kappa = M/T^2$.

Equation (15) can also be expressed as follows:

$$q(i) = \underset{q \in \mathcal{A}(q^*(i))}{\text{argmin}} |q - q(i-1)| \quad (22)$$

where

$$\mathcal{A}(q^*(i)) = \{q \in \mathbb{R} \mid -F/\kappa < q - p^*(i) < F/\kappa\}. \quad (23)$$

Here, $\mathcal{A}(q^*(i))$ can be viewed as the set of the possible values for $q(i)$, and (22) shows that the value $q(i)$ is determined so that it minimizes the distance from $q(i-1)$.

B. Plasticity-Based Virtual Fixtures

The use of the simulated plasticity for a virtual fixture is now presented. Its basic concept is illustrated in Fig. 3. We here consider two types of virtual fixtures: bilateral and unilateral. A bilateral one acts to prevent the tool from departing from a reference surface (or curve). A unilateral one acts to prevent the tool from entering a forbidden region, which should not be entered. We also refer to the boundary of the unilateral virtual fixture as a reference surface. A plasticity-based virtual fixture generates a large resistance force when the user is moving deeper into the forbidden region. Otherwise, it generates a small resistance force for helping stable task execution by canceling unintended tremors or disturbances, as demonstrated in [8]. The force always opposes the velocity and thus it is passive.

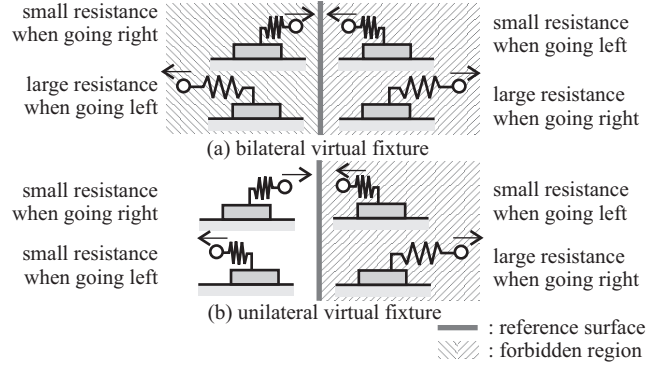


Fig. 3. Plasticity-based virtual fixtures.

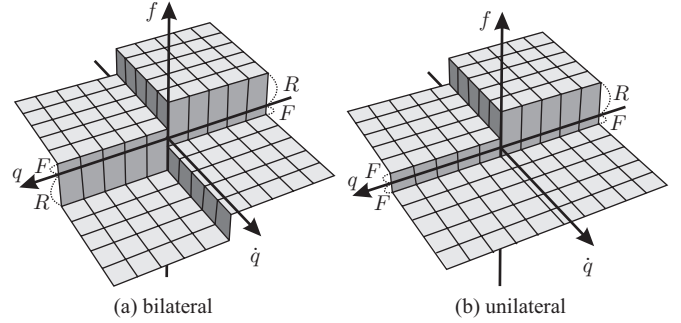


Fig. 4. The relations between f , q , and \dot{q} with a bilateral virtual fixture (a) and a unilateral virtual fixture (b).

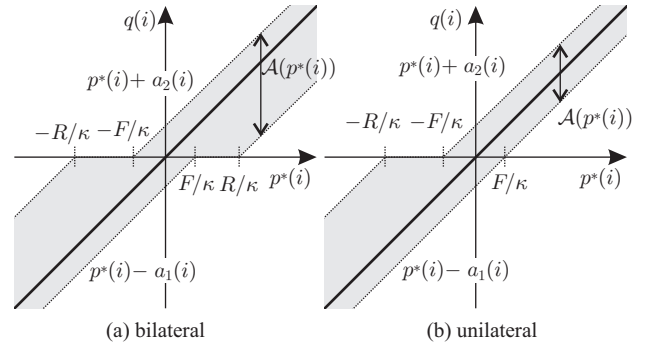


Fig. 5. The set $\mathcal{A}(p^*(i))$ of possible new proxy positions $q(i)$ in a bilateral virtual fixture (a) and a unilateral virtual fixture (b).

Let $q = 0$ be the reference surface in the one-dimensional space. Then, the force f from a bilateral virtual fixture can be written as follows:

$$f = -\text{gsat}(\text{gsat}(-R, q, -F), \dot{q}, \text{gsat}(F, q, R)) \quad (24)$$

where $R \gg F > 0$. A unilateral virtual fixture, on the other hand, can be described as follows:

$$f = -\text{gsat}(\text{gsat}(-R, q, -F), \dot{q}, F) \quad (25)$$

where $\{q \in \mathbb{R} \mid q < 0\}$ is assumed to be the forbidden region. The relations (24) and (25) are illustrated in Fig. 4(a) and Fig. 4(b), respectively. Notice that f can take intermediate values other than $\pm R$ or $\pm F$ when $q = 0$ or $\dot{q} = 0$.

The plastic characteristics of (24) and (25) can be implemented in discrete-time systems by replacing f by $\kappa(q(i) - p^*(i))$ and \dot{q} by $(q(i) - q(i-1))/T$, as demonstrated in section II-A. After some derivation, this variable transformation

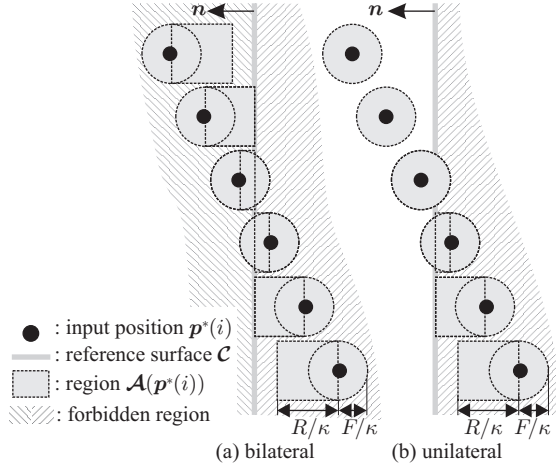


Fig. 6. Geometric representations of the set $\mathcal{A}(\mathbf{p}^*(i))$ for a bilateral virtual fixture (a) and a unilateral virtual fixture (b).

onto (24) yields

$$\mathbf{q}(i) = \mathbf{p}^*(i) + \text{gsat}(-a_1(i), \mathbf{q}(i-1) - \mathbf{p}^*(i), a_2(i)) \quad (26)$$

where

$$a_1(i) = \text{gsat}(F/\kappa, \mathbf{p}^*(i), R/\kappa) \quad (27)$$

$$a_2(i) = \text{gsat}(F/\kappa, -\mathbf{p}^*(i), R/\kappa). \quad (28)$$

In the same manner, (25) is transformed into the same form (26) but where $a_1(i)$ and $a_2(i)$ have the following definitions:

$$a_1(i) = F/\kappa \quad (29)$$

$$a_2(i) = \text{gsat}(F/\kappa, -\mathbf{p}^*(i), R/\kappa). \quad (30)$$

In both cases, the set $\mathcal{A}(\mathbf{p}^*(i))$, which is the set of the possible values for $\mathbf{q}(i)$, can be represented as

$$\mathcal{A}(\mathbf{q}^*(i)) = \{\mathbf{q} \in \mathbb{R} \mid -a_1(i) < \mathbf{q} - \mathbf{p}^*(i) < a_2(i)\}, \quad (31)$$

which is shown in Fig. 5.

III. MULTIDIMENSIONAL VIRTUAL FIXTURES

A. Geometric Representation of Anisotropic Plasticity

The previous section showed that the plasticity in one-dimensional case is represented by a set of possible proxy positions $\mathcal{A}(\mathbf{p}^*(i))$, of which a larger size indicates a larger yield force. This section extends this idea to represent anisotropic plasticity in n -dimensional space. Hereafter we use boldface symbols to denote vectors correspondent to scalars in section II. The new proxy position $\mathbf{q}(i)$ is determined to be the position nearest to the previous proxy position $\mathbf{q}(i-1)$ within the set $\mathcal{A}(\mathbf{p}^*(i))$, which depends on the input position $\mathbf{p}^*(i)$. This rule is concisely described as

$$\mathbf{q}(i) = \underset{\mathbf{q} \in \mathcal{A}(\mathbf{p}^*(i))}{\text{argmin}} \|\mathbf{q} - \mathbf{q}(i-1)\|. \quad (32)$$

This section discusses how the set $\mathcal{A}(\mathbf{p}^*(i))$ should be defined to produce plasticity-based virtual fixtures and how the new proxy position $\mathbf{q}(i)$ should be chosen to satisfy (32).

We start our discussion from a simple case in which the reference surface \mathcal{C} is defined as an $(n-1)$ -dimensional

subspace in the n -dimensional space: \mathcal{C} is a flat plane in a three-dimensional space or is a straight line in a two-dimensional space. The tool should be constrained on \mathcal{C} if it is bilateral but \mathcal{C} is the boundary of a forbidden region if it is unilateral. For producing such virtual fixtures, we propose to use the anisotropic plasticity that is geometrically represented in Fig. 6, which can be described as follows:

$$\mathcal{A}(\mathbf{p}^*(i)) = \mathcal{A}_F(\mathbf{p}^*(i)) \cup \mathcal{A}_R(\mathbf{p}^*(i)) \quad (33)$$

where

$$\mathcal{A}_F(\mathbf{p}^*(i)) = \{\mathbf{q} \in \mathbb{R}^n \mid \|\mathbf{q} - \mathbf{p}^*(i)\| \leq F/\kappa\} \quad (34)$$

$$\mathcal{A}_R(\mathbf{p}^*(i)) = \{\mathbf{q} \in \mathbb{R}^n \mid \|\mathbf{n} \times (\mathbf{q} - \mathbf{p}^*(i))\| \leq F/\kappa \\ \wedge -a_1(i) < \mathbf{n}^T(\mathbf{q} - \mathbf{p}^*(i)) \leq a_2(i)\} \quad (35)$$

and

$$a_1(i) = \begin{cases} \text{gsat}(0, \mathbf{n}^T(\mathbf{p}^*(i) - \mathbf{r}_C(i)), R/\kappa) & \text{if bi.} \\ 0 & \text{if uni.} \end{cases} \quad (36)$$

$$a_2(i) = \text{gsat}(0, -\mathbf{n}^T(\mathbf{p}^*(i) - \mathbf{r}_C(i)), R/\kappa). \quad (37)$$

Here, \mathbf{n} is the unit normal vector of \mathcal{C} projecting outward from the forbidden region in the unilateral case. (In the bilateral case, the direction does not matter.) The set $\mathcal{A}_F(\mathbf{p}^*(i))$ represents the circular (or spherical) region centering $\mathbf{p}^*(i)$. The set $\mathcal{A}_R(\mathbf{p}^*(i))$ is a rectangular (or cylindrical) region with a width (or diameter) $2F/\kappa$ and a length no larger than R/κ . The circular region $\mathcal{A}_F(\mathbf{p}^*(i))$ is for producing isotropic plastic response outside the forbidden region for helping stable task executions by canceling unintended tremors or disturbances. The rectangular region $\mathcal{A}_R(\mathbf{p}^*(i))$ is for producing a large yield force R to preventing the tool from entering the forbidden region.

Under the anisotropic plasticity based on $\mathcal{A}(\mathbf{p}^*(i))$, the new proxy position $\mathbf{q}(i)$ can be determined as follows:

$$\mathbf{q}(i) = \underset{\mathbf{q} \in \{\mathcal{A}_R(i), \mathcal{A}_F(i)\}}{\text{argmin}} \|\mathbf{q} - \mathbf{q}(i-1)\| \quad (38)$$

where

$$\mathbf{q}_R(i) = \underset{\mathbf{q} \in \mathcal{A}_R(\mathbf{p}^*(i))}{\text{argmin}} \|\mathbf{q} - \mathbf{q}(i-1)\| \quad (39)$$

$$\mathbf{q}_F(i) = \underset{\mathbf{q} \in \mathcal{A}_F(\mathbf{p}^*(i))}{\text{argmin}} \|\mathbf{q} - \mathbf{q}(i-1)\|. \quad (40)$$

Because $\mathcal{A}_F(\mathbf{p}^*(i))$ has a simpler form than $\mathcal{A}_R(\mathbf{p}^*(i))$, it is easier to calculate $\mathbf{q}(i)$ in the following procedure:

$$\mathbf{q}(i) = \underset{\mathbf{q} \in \mathcal{A}_R(\mathbf{p}^*(i))}{\text{argmin}} \|\mathbf{q} - \mathbf{q}(i-1)\|. \quad (41)$$

$$\text{IF } \|\mathbf{q}(i) - \mathbf{p}^*(i)\| < F/\kappa \text{ THEN} \quad (42)$$

$$\mathbf{q}(i) := \mathbf{p}^*(i) + \frac{\mathbf{q}(i) - \mathbf{p}^*(i)}{\max(1, \kappa\|\mathbf{q}(i) - \mathbf{p}^*(i)\|/F)} \quad (43)$$

$$\text{ENDIF} \quad (44)$$

Here, we use $:=$ to mean overwriting.

The problem still remaining is to solve (41), which relates to the rectangular region $\mathcal{A}_R(\mathbf{p}^*(i))$. In the direction normal to \mathcal{C} , the length of the region $\mathcal{A}_R(\mathbf{p}^*(i))$ is between 0 and R in the forbidden region and is 0 otherwise. Thus, the

proxy position in this direction can be updated in the same procedure as in the one-dimensional case with $F := 0$. Let us define the position $\mathbf{r}_C(i)$ as the point on \mathcal{C} closest to the input position $\mathbf{p}^*(i)$, i.e.,

$$\mathbf{r}_C(i) = \operatorname{argmin}_{\mathbf{r} \in \mathcal{C}} \|\mathbf{r} - \mathbf{p}^*(i)\|. \quad (45)$$

Then, we can see that $\mathbf{p}^*(i)$ and $\mathbf{q}(i)$ in the previous section correspond to $\mathbf{n}^T(\mathbf{p}^*(i) - \mathbf{r}_C(i))$ and $\mathbf{n}^T(\mathbf{q}(i) - \mathbf{r}_C(i))$, respectively. Therefore, (26) corresponds to

$$\mathbf{n}^T \mathbf{q}(i) = \mathbf{n}^T \mathbf{p}^*(i) + \operatorname{gsat}(-a_1(i), \mathbf{n}^T(\mathbf{q}(i-1) - \mathbf{p}^*(i)), a_2(i)) \quad (46)$$

where

$$a_1(i) = \begin{cases} \operatorname{gsat}(0, \mathbf{n}^T(\mathbf{p}^*(i) - \mathbf{r}_C(i)), R/\kappa) & \text{if bi.} \\ 0 & \text{if uni.} \end{cases} \quad (47)$$

$$a_2(i) = \operatorname{gsat}(0, -\mathbf{n}^T(\mathbf{p}^*(i) - \mathbf{r}_C(i)), R/\kappa). \quad (48)$$

Meanwhile, in the direction tangential to \mathcal{C} , we have to use

$$\mathbf{N}^T \mathbf{q}(i) = \mathbf{N}^T \mathbf{p}^*(i) + \frac{\mathbf{N}^T(\mathbf{q}(i-1) - \mathbf{p}^*(i))}{\max(1, \kappa \|\mathbf{N}^T(\mathbf{q}(i-1) - \mathbf{p}^*(i))\|/F)} \quad (49)$$

where \mathbf{N} is a column-full rank matrix that satisfies

$$\mathbf{N} \in \mathbb{R}^{n \times (n-1)}, \quad \mathbf{N}^T \mathbf{n} = \mathbf{o}, \quad \mathbf{N} \mathbf{N}^T + \mathbf{n} \mathbf{n}^T = \mathbf{I}. \quad (50)$$

Combining (46) and (49) yields

$$\begin{aligned} \mathbf{q}(i) &= \mathbf{N} \mathbf{N}^T \mathbf{q}(i) + \mathbf{n} \mathbf{n}^T \mathbf{q}(i) \\ &= \mathbf{p}^*(i) + \frac{(\mathbf{I} - \mathbf{n} \mathbf{n}^T)(\mathbf{q}(i-1) - \mathbf{p}^*(i))}{\max(1, \kappa \|\mathbf{n} \times (\mathbf{q}(i-1) - \mathbf{p}^*(i))\|/F)} \\ &\quad + \operatorname{ngsat}(-a_1(i), \mathbf{n}^T(\mathbf{q}(i-1) - \mathbf{p}^*(i)), a_2(i)) \end{aligned} \quad (51)$$

as the solution for (41). Here, we used the relation $\|\mathbf{N}^T \mathbf{x}\| = \|\mathbf{n} \times \mathbf{x}\|$ for all $\mathbf{x} \in \mathbb{R}^n$.

In conclusion, the computational procedure for producing a plasticity-based virtual fixture of an $(n-1)$ -dimensional subspace of the n -dimensional space is described as follows:

$$\mathbf{r}_C(i) = \operatorname{argmin}_{\mathbf{r} \in \mathcal{C}} \|\mathbf{r} - \mathbf{p}^*(i)\| \quad (52)$$

$$\mathbf{k}(i) = \mathbf{p}^*(i) - \mathbf{r}_C(i) \quad (53)$$

$$\mathbf{n}(i) = \pm \mathbf{k}(i) / \|\mathbf{k}(i)\| \quad /* \text{outward from forbidden region} */ \quad (54)$$

$$a_1(i) = \begin{cases} \operatorname{gsat}(0, \mathbf{n}(i)^T \mathbf{k}(i), R/\kappa) & \text{if bi.} \\ 0 & \text{if uni.} \end{cases} \quad (55)$$

$$a_2(i) = \operatorname{gsat}(0, -\mathbf{n}(i)^T \mathbf{k}(i), R/\kappa) \quad (56)$$

$$\mathbf{e}(i) = \mathbf{q}(i-1) - \mathbf{p}^*(i) \quad (57)$$

$$\begin{aligned} \mathbf{q}(i) &= \mathbf{p}^*(i) + \mathbf{n}(i) \operatorname{gsat}(-a_1(i), \mathbf{n}(i)^T \mathbf{e}(i), a_2(i)) \\ &\quad + \frac{(\mathbf{I} - \mathbf{n}(i) \mathbf{n}(i)^T) \mathbf{e}(i)}{\max(1, \kappa \|\mathbf{e}(i) \times \mathbf{n}(i)\|/F)} \end{aligned} \quad (58)$$

$$\text{IF } \|\mathbf{q}(i) - \mathbf{p}^*(i)\| < F/\kappa \text{ THEN} \quad (59)$$

$$\mathbf{q}(i) := \mathbf{p}^*(i) + \frac{\mathbf{e}(i)}{\max(1, \kappa \|\mathbf{e}(i)\|/F)} \quad (60)$$

$$\text{ENDIF.} \quad (61)$$

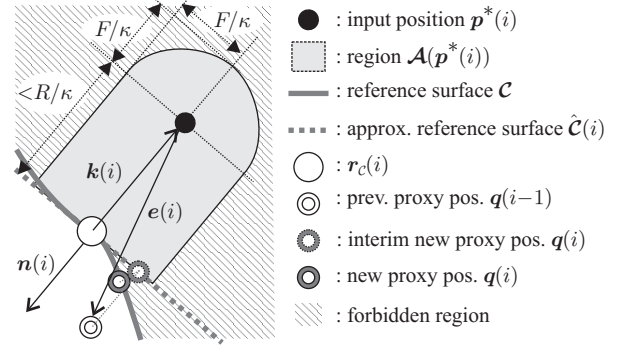


Fig. 7. Plasticity-based virtual fixture with curved reference surface.

B. Curved Reference Surface

When the reference surface \mathcal{C} is a curve or a curved surface, it is not easy to strictly calculate the new proxy position $\mathbf{q}(i)$ that satisfies (32). In such cases, we need to use an approximate solution for (32). One possible approach is to approximate \mathcal{C} by a tangential straight line (or plane) $\hat{\mathcal{C}}(i)$ near the point $\mathbf{r}_C(i)$. An interim value for the new proxy position on $\hat{\mathcal{C}}(i)$ can be obtained by the procedure of (52) to (61). The projection of the obtained position onto the reference surface \mathcal{C} can be an approximated solution for (32), as schematically illustrated in Fig. 7. This approach can be described as follows:

$$\text{RUN (52) TO (61)} \quad (62)$$

$$\text{IF } \mathbf{n}(i)^T \mathbf{k}(i) \notin \left\{ \begin{array}{l} [-R/\kappa, R/\kappa] \text{ if bi.} \\ [-R/\kappa, 0] \text{ if uni.} \end{array} \right\} \text{ THEN} \quad (63)$$

$$\text{IsOn}(i) = \text{FALSE} \quad (64)$$

$$\text{ELIF } (\mathbf{n}(i)^T \mathbf{k}(i))(\mathbf{n}(i)^T (\mathbf{k}(i) + \mathbf{e}(i))) \leq 0 \wedge \|\mathbf{q}(i) - \mathbf{p}^*(i)\| \geq F/\kappa \text{ THEN} \quad (65)$$

$$\text{IsOn}(i) = \text{TRUE} \quad (66)$$

$$\text{ELSE} \quad (67)$$

$$\text{IsOn}(i) = \text{IsOn}(i-1) \quad (68)$$

$$\text{END IF} \quad (69)$$

$$\text{IF IsOn}(i) = \text{TRUE THEN} \quad (70)$$

$$\mathbf{q}(i) := \operatorname{argmin}_{\mathbf{q} \in \mathcal{C}} \|\mathbf{q} - \mathbf{q}(i)\| \quad (71)$$

$$\text{END IF.} \quad (72)$$

Here, $\text{IsOn}(i)$ is a flag to indicate whether the proxy should be on the reference path \mathcal{C} or not at the time iT . The new proxy position $\mathbf{q}(i)$ is snapped onto \mathcal{C} by (71) if the flag $\text{IsOn}(i)$ is TRUE. The flag is switched from TRUE to FALSE if $\mathcal{A}_R(\mathbf{p}^*(i))$ is separated from $\hat{\mathcal{C}}(i)$, and is switched from FALSE to TRUE if $\mathcal{A}_R(\mathbf{p}^*(i))$ is in contact with $\hat{\mathcal{C}}(i)$, the previous proxy position $\mathbf{q}(i-1)$ and the input position $\mathbf{p}^*(i)$ are on different sides of $\hat{\mathcal{C}}(i)$, and the interim new proxy position $\mathbf{q}(i)$ is not included in $\mathcal{A}_F(\mathbf{p}^*(i))$.

IV. IMPLEMENTATION

The proposed algorithm was implemented in a Sensible PHANTOM Omni device, which was capable of three degree-of-freedom actuation and six degree-of-freedom

measurements. The sampling interval was set to be $T = 0.001$ sec. The measured position $\mathbf{p}(i)$ of the stylus of the device was converted into the input position $\mathbf{p}^*(i)$ by (17), and the proxy position $\mathbf{q}(i)$ was determined through the procedure of (62) to (72). The actuator force $\mathbf{f}(i)$ was determined by (19). The reference surface \mathcal{C} was chosen as a cylindrical surface with a radius of 40 mm whose axis coincides with the z -axis. The parameters were chosen as $K = 1.5$ N/mm, $B = 0.0015$ Ns/mm, $F = 0.5$ N, and $R = 3$ N. These values of K and B were chosen as high as possible without affecting the stability of the device. The value of F was chosen to produce a moderate frictional resistance for stable manual motion and R was chosen to produce a distinct resistance. The stylus (tool) was manually operated by an experimenter.

Fig. 8 shows the results obtained when \mathcal{C} was a bilateral virtual fixture. It is shown that the force \mathbf{f} is small when the tool is approaching to \mathcal{C} (a, e, and h) and is large when moving away from \mathcal{C} (d and g). The proxy is properly constrained on \mathcal{C} both when the stylus is pushed inward (b and i) and when pushed outward (c and f).

Fig. 9 shows the results obtained when \mathcal{C} was a unilateral virtual fixture whose forbidden region is inside of the cylinder. It is shown that the force \mathbf{f} is large when the tool is below the surface \mathcal{C} and is moving deeper (d) but is small when it is outside \mathcal{C} (a, c, and f) and when it is below the surface but moving shallower (e). The proxy is properly constrained on \mathcal{C} (b and g) when the tool is pushed onto the surface \mathcal{C} .

In both cases, the actuator force \mathbf{f} can take intermediate values smaller than F or R in the static friction state (i.e., when the tool is stationary). Thus, the presented algorithm does not cause chattering due to zero-velocity crossings. This property of the simulated plasticity is demonstrated in detail in our previous paper [5].

Although the demonstration here is limited to an impedance-type haptic interface, the proposed algorithm can also be used with admittance-type haptic interfaces, which have force sensors to measure forces applied from the user to the device. In this case, the measured force $\mathbf{h}(i)$ is used to derive the input position $\mathbf{p}^*(i)$ as described in (20), and the proxy position $\mathbf{q}(i)$ is determined through the procedure of (62) to (72). The device position is servo-controlled to follow the proxy position $\mathbf{q}(i)$.

V. CONCLUSIONS

This paper has presented an algorithm for always-passive virtual fixture based on position-dependent anisotropic plasticity. One advantage of our approach over viscosity-based virtual fixtures is that the tool does not move in the forbidden direction as long as the applied force is smaller than a predetermined magnitude. The proposed method was demonstrated through implementation experiments using an impedance-type haptic interface.

Future research will experimentally investigate the effect of the proposed approach on the human performance of precise manipulation tasks. Further variations of the reference

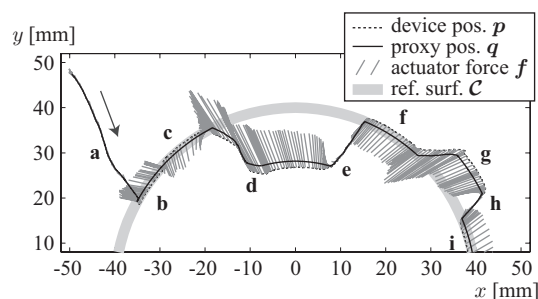


Fig. 8. Experimental results with a bilateral virtual fixture.

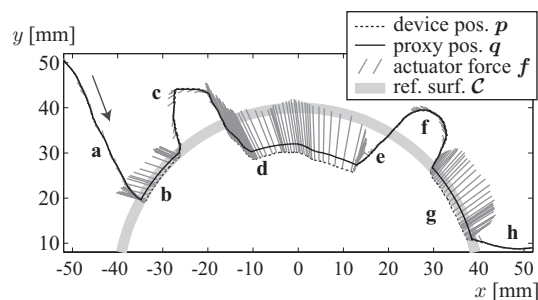


Fig. 9. Experimental results with a unilateral virtual fixture.

manifold \mathcal{C} will also need to be considered. In particular, this paper has not considered a curve (one-dimensional manifold) in three-dimensional space. Even for this case, a similar geometric approach using a set $\mathcal{A}(\mathbf{p}^*(i))$ will also be effective, but it should be investigated in the future study.

ACKNOWLEDGEMENT

We thank engineers at Toyota Motor Corporation who motivated this research.

REFERENCES

- [1] R. Taylor, P. Jensen, L. L. Whitcomb, A. Barnes, R. Kumar, D. Stoianovici, P. Gupta, Z. Wang, E. deJuan, and L. Kavoussi, "A steady-hand robotic system for microsurgical augmentation," *Int. J. of Robotics Research*, vol. 18, no. 12, pp. 1201–1210, 1999.
- [2] A. Bettini, P. Marayong, S. Lang, A. M. Okamura, and G. D. Hager, "Vision-assisted control for manipulation using virtual fixtures," *IEEE Trans. on Robotics*, vol. 20, no. 6, pp. 953–966, 2004.
- [3] J. J. Abbott and A. M. Okamura, "Virtual fixture architectures for telemanipulation," in *Proc. of the 2003 IEEE Int. Conf. on Robotics and Automation*, 2003, pp. 2798–2805.
- [4] H. Kang, Y. S. Park, T. F. Ewing, E. Faulring, and J. E. Colgate, "Visually and haptically augmented teleoperation in d&d tasks using virtual fixtures," in *Proc. of the American Nuclear Society 10th Int. Conf. on Robotics and Remote Systems for Hazardous Environments*, 2004, pp. 466–471.
- [5] R. Kikuuwe, N. Takesue, A. Sano, H. Mochiyama, and H. Fujimoto, "Admittance and impedance representations of friction based on implicit Euler integration," *IEEE Trans. on Robotics*, vol. 22, no. 6, pp. 1176–1188, 2006.
- [6] N. Takesue, R. Kikuuwe, A. Sano, H. Mochiyama, and H. Fujimoto, "Tracking assist system using virtual friction field," in *Proc. of the 2005 IEEE/RSJ Int. Conf. on Intelligent Robots and Systems*, 2005, pp. 2134–2139.
- [7] R. Kikuuwe and H. Fujimoto, "Incorporating geometric algorithms in impedance- and admittance-type haptic rendering," in *Proc. of the World Haptics Conf. 2007*, 2007, (to appear).
- [8] C. Richard and M. R. Cutkosky, "The effects of real and computer generated friction on human performance in a targeting task," in *Proc. of the ASME IMECE 2000 Symp. on Haptic Interfaces for Virtual Environments and Teleoperator Systems*, 2000, pp. 1101–1108.